Theory of Microphase Separation in Elastomers

Manu Mannattil,[1,2,3,*] Haim Diamant,[1,3] and David Andelman[2,3]
[1]*School of Chemistry, Tel Aviv University, Ramat Aviv, Tel Aviv 69978, Israel*
[2]*School of Physics and Astronomy, Tel Aviv University, Ramat Aviv, Tel Aviv 69978, Israel*
[3]*Center for Physics and Chemistry of Living Systems, Tel Aviv University, Tel Aviv 69978, Israel*

(Received 8 December 2024; revised 4 May 2025; accepted 11 August 2025; published 3 September 2025)

Inspired by recent experiments, we present a phase-field model of microphase separation in an elastomer swollen with a solvent. The imbalance between the molecular scale of demixing and the mesoscopic scale beyond which elasticity operates produces effective long-range interactions, forming stable finite-sized domains. Our predictions concerning the dependence of the domain size and transition temperature on the stiffness of the elastomer are in good agreement with the experiments. Analytical phase diagrams, aided by numerical findings, capture the richness of the microphase morphologies, paving the way to create stable, patterned elastomers for various applications.

DOI: 10.1103/5q7m-3fpn

Introduction—The interplay between elasticity and phase separation has been widely explored in various contexts since Cahn's classic work from the 1960s on spinodal decomposition [1]. For example, a mismatch in the constituents' elastic moduli in metallic alloys can either hinder or speed up phase separation [2]. Similarly, elasticity regulates the morphology of the phase-separated domains in gels [3–5] and liquid-crystalline fluids [6], which can lead to intricate patterns. Besides, mounting evidence now indicates that phase separation and elasticity are both crucial to the development of many membraneless organelles within biological cells, rekindling interest in the topic [7–11]. To sidestep the complexities of the biological world, several experiments have been conducted with synthetic, *in vitro* model systems in the past few years [12–16]. The results of these experiments, along with related theoretical work [17–23], once again emphasize the influence of elasticity on phase separation in soft matter systems.

A recent experiment showed elasticity-controlled microphase separation to be a highly effective technique for generating patterned elastomers with complex morphologies [24]. In the study, a temperature quench is used to trigger microphase separation in elastomers swollen with a solvent. The results are reminiscent of older observations of phase separation and critical density fluctuations in swollen gels as the temperature is lowered [25–28]. In the new experiments, however, the elastomer does not fully phase separate from the solvent, and instead forms stable bicontinuous microstructures or droplets whose sizes are determined by the stiffness of the elastomer. This microphase separation plausibly arises because of a pronounced difference in the length scales at which thermodynamics and elasticity operate [24]. This is unlike previous examples, where patterned phases were primarily seen in systems with anisotropic elasticity or external stresses [29] or involving nontrivial phenomena such as cavitation [18,30].

In this Letter, we introduce a phase-field model that captures the key features of microphase separation in swollen elastomers in the limit of weak segregation. Recent theoretical work [31], also inspired by the aforementioned experiments, has demonstrated that the length-scale discrepancy between elasticity and thermodynamics in elastomers can be resolved using nonlocal theories of elasticity [32–34]. Nonlocal approaches have also been employed in other systems with scale-dependent phenomena, such as certain porous materials [35] and DNA elasticity [36].

The stiffness of elastomers arise primarily due to strain-induced changes in the configurational entropy of polymer chains [37–39]. Our scaling results for the domain size and microphase separation temperature, obtained by using results from rubber (entropic) elasticity and incorporating nonlocal effects, agree with the experimental observations. We also highlight the diversity of the microphase morphologies by constructing a phase diagram and supplementing it with numerical results. Put together, our findings underscore an intricate coupling between thermodynamics and elasticity, opening up novel ways to produce patternable materials for various purposes.

Model—We consider a charge-neutral elastomer consisting of a cross-linked polymer network isotropically swollen with a solvent. Polymer-solvent interaction occurs over typical intermolecular distances (e.g., the size of the solvent molecules). On the other hand, the elastic response of the elastomer stems entirely from the underlying polymer network, which has a much larger, usually mesoscopic, characteristic length scale (Fig. 1). Deformations of the

*Contact author: manu.mannattil@posteo.net

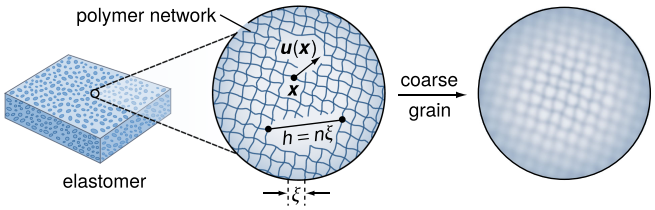

FIG. 1. Displacements $\boldsymbol{u}(\boldsymbol{x})$ occurring below a characteristic length scale h do not stress the elastomer significantly. Using a coarse-grained strain field $\bar{\boldsymbol{\varepsilon}}$, such displacements are "blurred away" and filtered out. In our model, we choose h as a multiple $n\xi$ of the end-to-end distance ξ between adjacent cross-links of the polymeric network within the elastomer.

elastomer occurring below this length scale should not engender a significant elastic response. Elastomers can undergo large deformations during swelling, and they are customarily studied using nonlinear elasticity [40]. However, once the elastomer is completely swollen, further elastic deformations are well described using linear elasticity in terms of a three-dimensional (3D) displacement field $\boldsymbol{u}(\boldsymbol{x})$ defined over points $\boldsymbol{x}$ on the elastomer [41]. The resulting strain field is $\boldsymbol{\varepsilon} = \frac{1}{2}[\boldsymbol{\nabla u} + (\boldsymbol{\nabla u})^{\mathsf{T}}]$, with $(\boldsymbol{\nabla u})^{\mathsf{T}}$ being the transpose of $\boldsymbol{\nabla u}$.

For a precise description of thermodynamic interactions caused by compositional changes in the elastomer, the continuum fields $\boldsymbol{u}$ and $\boldsymbol{\varepsilon}$ must both be defined at molecular length scales. However, only those deformations occurring above a much larger length scale stress the elastomer substantially. To address this, we consider a constitutive stress-strain relationship of the form

$$\boldsymbol{\sigma}(\boldsymbol{\varepsilon}) = \lambda(\mathrm{tr}\,\bar{\boldsymbol{\varepsilon}})\mathbb{1} + 2\mu\bar{\boldsymbol{\varepsilon}}, \tag{1}$$

where λ and μ are the Lamé parameters, $\mathbb{1}$ is the 3×3 identity matrix, and $\mathrm{tr}\,\bar{\boldsymbol{\varepsilon}}$ denotes the trace of a coarse-grained strain $\bar{\boldsymbol{\varepsilon}}$, defined by

$$\bar{\boldsymbol{\varepsilon}}(\boldsymbol{x}) = \int \mathrm{d}^3x' K_h(\boldsymbol{x}-\boldsymbol{x}')\boldsymbol{\varepsilon}(\boldsymbol{x}'). \tag{2}$$

Here $K_h(\boldsymbol{x}-\boldsymbol{x}')$ is an isotropic, scalar kernel that depends only on the distance $|\boldsymbol{x}-\boldsymbol{x}'|$ between two points $\boldsymbol{x},\boldsymbol{x}'$ in space. For concreteness, we use a normalized Gaussian kernel $K_h(\boldsymbol{x}) = (4\pi h^2)^{-3/2}\mathrm{e}^{-|\boldsymbol{x}|^2/(4h^2)}$, with h being a suitable mesoscopic length scale that controls the extent of coarse-graining. Nonetheless, as we demonstrate in Supplemental Material (SM) [42], our results are independent of our choice for this kernel.

The stress $\boldsymbol{\sigma}$ computed using Eqs. (1) and (2) models the correct elastic response of the elastomer, while simultaneously allowing us to use the strain $\boldsymbol{\varepsilon}$ to capture compositional changes at molecular length scales. This model is a particular instance of the Eringen framework [32–34] of nonlocal elasticity, and it leads to an elastic energy density $w(\boldsymbol{\varepsilon})$ of the form

$$w(\boldsymbol{\varepsilon}) = \frac{\lambda}{2}(\mathrm{tr}\,\boldsymbol{\varepsilon})(\mathrm{tr}\,\bar{\boldsymbol{\varepsilon}}) + \mu\mathrm{tr}\,(\boldsymbol{\varepsilon}\bar{\boldsymbol{\varepsilon}}), \tag{3}$$

obtained by contracting the strain $\boldsymbol{\varepsilon}$ with the stress $\boldsymbol{\sigma}$ in Eq. (1) expressed in terms of $\bar{\boldsymbol{\varepsilon}}$. As the kernel K_h is positive definite and normalized, $w(\boldsymbol{\varepsilon})$ remains positive, bounded from below, and reduces to the usual Hookean energy density in the limit $h \to 0$.

Let the elastomer be isotropically swollen initially at a temperature T with a constant volume fraction ϕ_0 of the polymer network. Compositional changes that occur as the temperature is lowered cause the local network volume fraction $\phi(\boldsymbol{x})$ at a point $\boldsymbol{x}$ to deviate from ϕ_0. The grand-canonical free energy of the elastomer is then given by

$$\mathscr{F}[\psi,\boldsymbol{\varepsilon}] = \int \mathrm{d}^3x\left[f(\psi) + \frac{1}{2}\kappa|\boldsymbol{\nabla}\psi|^2 + w(\boldsymbol{\varepsilon}) - \eta\psi\right]. \tag{4}$$

Here we have defined the order parameter (phase field) $\psi(\boldsymbol{x}) = \phi(\boldsymbol{x}) - \phi_*$ assuming that the homogeneous system has a "critical" point (ϕ_*, T_*), and take the free-energy density $f(\psi)$ to be in a Landau form

$$f(\psi) = \frac{1}{2}a(T-T_*)\psi^2 + \frac{1}{4}b\psi^4, \tag{5}$$

with a and b being positive phenomenological constants. Contributions from polymer-solvent mixing are included in this phenomenological $f(\psi)$, with the ψ^4 term playing an additional role in stabilizing phase separation. For polymer networks cross-linked in solution, the critical temperature T_* is likely to be close to the theta temperature before cross-linking [69]. Similar free-energy densities have been used to model swelling and deswelling of gels [70–73]. Also included in Eq. (4) is the elastic energy density $w(\boldsymbol{\varepsilon})$ and a gradient-squared term with an interfacial parameter $\kappa > 0$ to penalize spatial variations in ψ. Finally, η is a Lagrange multiplier to constrain the mean value of ψ to $\psi_0 = \phi_0 - \phi_*$, thereby conserving the total volume of the polymer network.

For small deformations of the elastomer close to the critical point, the strain $\boldsymbol{\varepsilon}$ and the order parameter ψ are related by a material conservation relation (SM [42]),

$$\mathrm{tr}\,\boldsymbol{\varepsilon} = \boldsymbol{\nabla}\cdot\boldsymbol{u} \approx -\phi_*^{-1}\psi. \tag{6}$$

Compositional changes in the polymer volume fraction during temperature quenches arise primarily via solvent diffusion. This allows us to disregard shear deformations and use Eqs. (3) and (6) to write the total elastic energy as a binary interaction in ψ mediated by the coarse-graining kernel K_h.

For linear stability analysis of Eq. (4), we express the order parameter $\psi(\boldsymbol{x})$ and the kernel $K_h(\boldsymbol{x})$ in terms

of their Fourier transforms, $\psi_{\boldsymbol{q}} = \int \mathrm{d}^3x\, \mathrm{e}^{-i\boldsymbol{q}\cdot\boldsymbol{x}}\psi(\boldsymbol{x})$ and $K_h(\boldsymbol{q}) = \mathrm{e}^{-h^2q^2}$. Upon expressing the quadratic part of the total free energy in Fourier space, we find (SM [42])

$$\mathscr{F}[\psi] = \frac{1}{2}\int \frac{\mathrm{d}^3q}{(2\pi)^3}\psi_{-\boldsymbol{q}}F_{\boldsymbol{q}}\psi_{\boldsymbol{q}} + \int \mathrm{d}^3x\left(\frac{1}{4}b\psi^4 - \eta\psi\right), \quad (7)$$

where $F_{\boldsymbol{q}}$ is the Fourier transform of the effective binary interaction for ψ given by

$$F_{\boldsymbol{q}} = a(T - T_*) + \kappa q^2 + M\mathrm{e}^{-h^2q^2}. \quad (8)$$

Here $q = |\boldsymbol{q}|$ and $M = (\lambda + 2\mu)/{\phi_*}^2$ is the rescaled longitudinal modulus [74,75] of the swollen elastomer.

The second term in Eq. (8), which favors long-range (small q) modulations in ψ, measures the energy cost to create interfaces. Meanwhile, the elastic term $M\mathrm{e}^{-h^2q^2}$ favors short-range (large q) modulations. Hence, we expect the emergence of a stable, spatially modulated phase at an intermediate length scale, provided that the elastic term is adequately large. The characteristic size of the modulated phase scales as $\Lambda \sim 2\pi {q_\mathrm{m}}^{-1}$, where q_m is the wave number at which $F_{\boldsymbol{q}}$ acquires its minimum. From Eq. (8), we see that $F_{\boldsymbol{q}}$ has a minimum at a nonzero q_m given by

$$q_\mathrm{m}^2 = h^{-2}\ln\gamma, \quad (9)$$

only if the dimensionless parameter $\gamma = Mh^2/\kappa > 1$. The parameter γ, which measures the relative importance of elastic and interfacial effects, is analogous to the (inverse) elastocapillary number [20,76] and the Lifshitz point [77] of Eq. (7) is located at $\gamma = 1$ (SM [42]). If the elastic energy cost exceeds the cost to form interfaces ($\gamma > 1$), the system can minimize its total energy by creating many stable, finite-sized domains, resulting in microphase separation. Note that if $h = 0$ in Eq. (2) and the system exhibits a local elastic response, we can recover known results for swollen polymer networks from the free energy in Eq. (7), such as the onset of spinodal decomposition at temperatures where the osmotic longitudinal modulus vanishes, negative Poisson's ratio, etc. [78] (SM [42]).

During a temperature quench from the uniform phase with $\psi(\boldsymbol{x}) = \psi_0$, the onset of microphase separation is indicated by linear instability in the order-parameter fluctuations. Upon expressing $\psi(\boldsymbol{x}) = \psi_0 + \delta\psi(\boldsymbol{x})$ and expanding the free energy in Eq. (7) up to $\mathcal{O}(\delta\psi^2)$ in the fluctuations $\delta\psi(\boldsymbol{x})$, we determine that the instability arises at a temperature where $F_{\boldsymbol{q}} = -3b{\psi_0}^2$ and $q = q_\mathrm{m}$. This provides an estimate for the temperature T_micro at which microphase separation begins, which we find to be

$$T_\mathrm{micro}(\psi_0) = T_* - a^{-1}\left[3b{\psi_0}^2 + M\gamma^{-1}(1 + \ln\gamma)\right]. \quad (10)$$

Clearly, T_micro decreases linearly with the modulus M, showing that deeper temperature quenches are required to induce microphase separation in stiffer elastomers.

Comparison to experiments—Polydimethylsiloxane (PDMS) elastomers, such as the ones used in the experiments in Ref. [24], are susceptible to chain entanglement effects that can alter their elastic response substantially, particularly at low crosslink densities [79–82]. However, based on the observed variation of the Young's modulus with cross-link density (detailed in the SM [42]), we judge entanglement effects to be negligible, enabling us to use classical rubber elasticity theory in our analysis.

Apart from the intermolecular distance, a relevant length scale in elastomers is the root-mean-square end-to-end distance ξ of the strands between adjacent cross-links in the polymer network [83–86] (Fig. 1). Taking each strand to be a freely jointed chain with a Flory ratio C_∞ [37], composed of N repeat units of length ℓ, we have $\xi^2 \sim \frac{1}{2}C_\infty N\ell^2$ [38,86]. Here the factor of $\frac{1}{2}$ is an estimate assuming the network junctions have tetrafunctional connectivity. If the strands and the repeat units have molecular masses m_s and m_r, respectively, then $N = m_\mathrm{s}/m_\mathrm{r}$. Assuming that the elastomer has a mass density ρ, its Young's modulus in the dry state is $Y = 3\rho k_\mathrm{B}T/2m_\mathrm{s}$ [39]. Using this expression to write m_s and N in terms of Y, we find that the end-to-end distance scales as [84,85]

$$\xi \sim (3B/Y)^{1/2}, \quad (11)$$

where $B = C_\infty\rho\ell^2k_\mathrm{B}T/(4m_\mathrm{r})$ is a material-dependent parameter, with k_B being the Boltzmann constant. See SM [42] for further details. For PDMS elastomers we find $B = 0.006\ \mathrm{kPa}\,\mu\mathrm{m}^2$, which gives $\xi \sim 5 - 50$ nm for the experimental range of $Y \sim 10 - 800$ kPa. Compared to ξ, the intermolecular length scale ($\sim\ell$) is of the order of a few Å. The polymer network within the elastomer can be treated as an elastic continuum only at length scales much larger than ξ, but proportional to it. For this reason, we take the coarse-graining length scale to be $h = n\xi$. Here, the phenomenological factor n can be interpreted as the average number of crosslinks we coarse grain over in each direction (Fig. 1). Its value depends on the kernel used in Eq. (2), with wider, long-range kernels giving smaller values for n.

In order to estimate the domain size Λ of the microphases, we note that the rescaled longitudinal modulus M of a swollen elastomer is related to its dry Young's modulus Y via $M \sim \frac{1}{3}{\phi_*}^{-5/3}Y$ [28,42]. Interface formation occurs at intermolecular length scales, so we estimate the interfacial parameter as $\kappa \sim k_\mathrm{B}T/\ell$ [87]. With the choice $h = n\xi$, the parameter γ is independent of Y, and using Eqs. (9) and (11) we find the scaling

$$\Lambda \sim 2\pi\left[\frac{3Bn^2}{Y\ln\left(Bn^2\kappa^{-1}\phi_*^{-5/3}\right)}\right]^{1/2}. \quad (12)$$

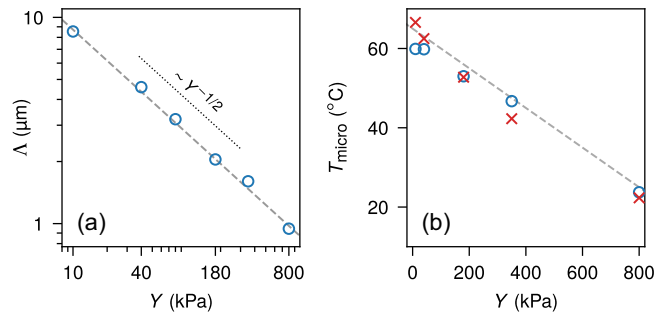

FIG. 2. (a) Domain size Λ as a function of the Young's modulus Y of the dry elastomer (log-log plot). The circles indicate experimental values of Λ for PDMS elastomers from Ref. [24], showing the scaling $\Lambda \sim Y^{-1/2}$. The dashed line represents the prediction from Eq. (12) with $\kappa = 0.013\ \mathrm{kPa\,\mu m^2}$ and fitting parameters $n = 110$, $\phi_* = 0.2$. (b) Decrease in the microphase separation temperature T_{micro} with Y. The circles show the experimental values of T_{micro} for an initial swelling temperature of 60 °C [24]. The crosses represent T_{micro} estimated from Eq. (10) using experimental values of the mean polymer volume fraction ϕ_0, with the dashed guideline illustrating the inearity between T_{micro} and Y. Other fitting parameters are $a = 0.025\ \mathrm{kPa\,K^{-1}}$, $b = 2$ kPa, and $T_* = 70$ °C.

The scaling $\Lambda \sim Y^{-1/2}$ above is markedly different from what one would expect on dimensional grounds alone (the so-called rheological mesh size of polymer networks that scales as $(k_{\mathrm{B}}T/Y)^{1/3}$ [88,89]). In Fig. 2(a), we compare the experimental results and Eq. (12) and find good agreement between the two. Furthermore, as we see from Fig. 2(b), the microphase separation temperature T_{micro} linearly decreases with Y, which is consistent with the prediction of Eq. (10). Using the T_{micro} data, one can estimate the parameters (ϕ_*, T_*) appearing in Eq. (5). We show in the SM [42] that these scalings for Λ and T_{micro} are agnostic to the choice of the kernel K_h in Eq. (2).

Close to the critical point, the microphase domain boundaries are diffuse (weak segregation), and they are well approximated as modulations in the order parameter ψ with a wave number $q = q_{\mathrm{m}}$ [90,91]. A phase diagram in the (ϕ_0, T) plane constructed using this one-mode approximation is presented in Fig. 3(a), with the analytical steps detailed in SM [42]. For simplicity, we have only examined 2D modulations in the phase diagram. Nonetheless, it shows excellent agreement with the equilibrium phases found by numerically minimizing the free energy in 3D [Figs. 3(b) and 3(c)]. Near the critical point, there are three distinct phases: a uniform phase, a droplet (hexagonal) phase consisting of solvent-rich droplets embedded within the elastomer, and a stripe phase composed of alternating solvent-rich and solvent-deficient layers. An "inverted" droplet phase also appears at low ϕ_0.

In Fig. 3(a), the first-order phase-transition curves that divide the different phases converge at a critical point T'_*, where a second-order transition between the uniform and the stripe phase is possible. The phase diagram has the

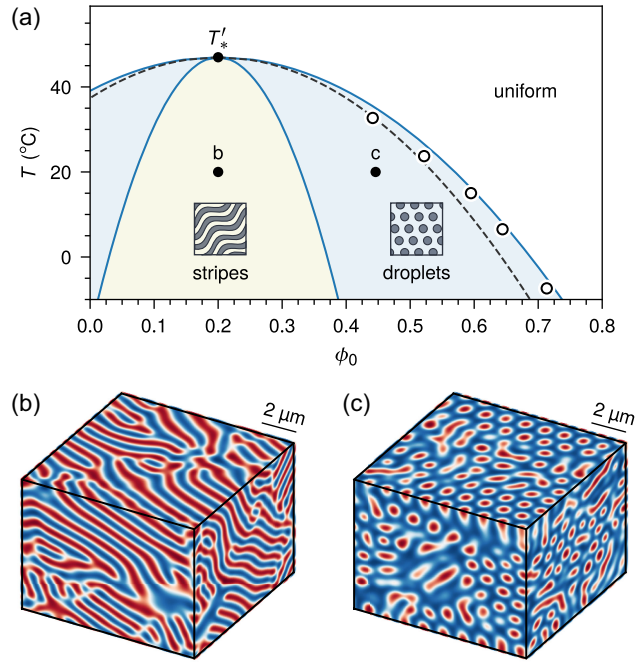

FIG. 3. (a) Phase diagram in the (ϕ_0, T) plane for an elastomer with a dry Young's modulus $Y = 800$ kPa. Here T is the temperature, and ϕ_0 is the mean polymer volume fraction. Other parameters are the same as in Fig. 2. The solid curves show the phase boundaries (binodals). Phase coexistence regions are not depicted as they are very narrow. The dashed curve depicts the microphase separation temperature $T_{\mathrm{micro}}(\psi)$ from Eq. (10) with a shifted critical temperature $T'_* = T_{\mathrm{micro}}(0)$. The open circles represent experimental results from Ref. [24]. (b),(c) Equilibrium morphologies of the elastomer obtained by numerically minimizing the free energy, Eq. (7), with the corresponding (ϕ_0, T) values marked in (a). Solvent-rich ($\phi < \phi_0$) and solvent-deficient ($\phi > \phi_0$) regions are highlighted in red and blue, respectively.

same topology as phase diagrams for block copolymers [92,93] and other systems displaying modulated phases [94–97], which are often characterized by a Landau–Brazovskii free energy. We show in SM [42] that the free energy in Eq. (7) can be simplified to this form, explaining the generic nature of the phase diagram, which also has regions of phase coexistence [42]. However, for the experimental parameter ranges used here, the widths of these regions are very small, and therefore are not depicted. The absence of substantial regions of phase coexistence may account for the apparent lack of hysteresis seen in the experiments [24].

The phase diagram in Fig. 3(a) shows good agreement with the experimental results and predicts the onset of microphase separation well. Experimentally, droplets are seen in soft elastomers with $Y \lesssim 40$ kPa. Only bicontinuous structures (different from stripes and droplets) are observed in stiffer elastomers. However, because of the generic topology of the theoretical phase diagram, irrespective of the stiffness, we expect the droplet phase to always appear first during an off-critical temperature

quench. This suggests that some other mechanism is responsible for the emergence of bicontinuous structures in stiffer samples, e.g., shear deformations or nonlinear effects, which we have neglected. Further consistency with experiments is seen upon examining the static structure factor, found using Eq. (7) as $S(q) \sim F_{\boldsymbol{q}}^{-1}$. It peaks at $q = q_{\mathrm{m}}$, given in Eq. (9), and explains the smooth increase of the scattering intensity at a fixed q during a temperature quench as seen in the experiments (SM [42]).

Summary and outlook—Using a phase-field model for swollen elastomers, we have predicted the possibility of a microphase separation arising from an imbalance between the intermolecular length scale and the mesoscopic coarseness of network elasticity. The elastomer remains stable with an intrinsically selected length scale if the free-energy contribution from the network elasticity is adequately large compared to the interfacial energy costs. Our scaling predictions for the domain size Λ and the microphase separation temperature T_{micro} as a function of the elastic moduli are consistent with recent experimental observations [24].

As the number of repeat units N between the crosslinks follows the scaling $N \sim Y^{-1}$, we find $\Lambda \sim N^{1/2}$ and a linear dependence between T_{micro} and N^{-1}. Intriguingly, similar scaling behaviors have been experimentally observed in crosslinked polymer blends [98,99] and were predicted earlier by de Gennes [100] using a phenomenological model that draws an analogy to electrostatics. The similarity in the scaling suggests that the internal elastic response of these blends may be nonlocal.

Our use of nonlocal elasticity was motivated by a recent theoretical study [31] inspired by the same experiments on elastomers. In this study, a one-dimensional (1D) nonlocal model was used to obtain the scaling $\Lambda \sim Y^{-1/2} h^{1/2} \kappa^{1/4}$ in the strong-segregation limit, taking the nonlocality scale h and the Young's modulus Y to be independent. This scaling is different from our 3D result for weak segregation, Eq. (12), which also takes into account the inter-dependence of h and Y, incorporating results from rubber elasticity. Furthermore, our model predicts a first-order transition from the uniform phase to various patterned phases. Conversely, in the 1D nonlocal model, a line of second-order transitions was predicted for large Y based on detailed numerical analyses [31]. Differences in the dimensionalities of the two models may explain this discrepancy (SM [42]).

Microphase separation in elastomers closely resembles that in block copolymers and other systems exhibiting modulated phases [90]. As we discuss in SM [42], we expect it to be a rich source of related phenomena such as fluctuation-induced first-order transitions [93,101], Lifshitz behavior [102,103], microemulsion phases, etc. [104,105]. Other experimentally relevant theoretical questions include the kinetics of phase separation [70,106], effect of quenched impurities and network heterogeneities [107–109], volume phase transitions [110,111], etc. Finally, extensions of our theory to ternary systems in the strong segregation regime could help elucidate the non-power-law scaling of the domain size observed in earlier experiments [12].

Acknowledgments—We thank Ram Adar, Enrico Carlon, Amit Kumar, Chengjie Luo, L. Mahadevan, Yicheng Qiang, Yitzhak Rabin, Sam Safran, Lev Truskinovsky, and David Zwicker for useful conversations. M. M. acknowledges partial support through the Bloomfield Fellows Program at Tel Aviv University. H. D. acknowledges support from the Israel Science Foundation (ISF Grant No. 1611/24). D. A. acknowledges support from the Israel Science Foundation (ISF Grant No. 226/24).

[1] J. W. Cahn, On spinodal decomposition, Acta Metall. **9**, 795 (1961).
[2] P. Fratzl, O. Penrose, and J. L. Lebowitz, Modeling of phase separation in alloys with coherent elastic misfit, J. Stat. Phys. **95**, 1429 (1999).
[3] Y. Rabin and S. Panyukov, Scattering profiles of charged gels: Frozen inhomogeneities, thermal fluctuations, and microphase separation, Macromolecules **30**, 301 (1997).
[4] O. Peleg, M. Kröger, I. Hecht, and Y. Rabin, Filamentous networks in phase-separating two-dimensional gels, Europhys. Lett. **77**, 58007 (2007).
[5] J. Dervaux and M. B. Amar, Mechanical instabilities of gels, Annu. Rev. Condens. Matter Phys. **3**, 311 (2012).
[6] J.-C. Loudet, P. Barois, and P. Poulin, Colloidal ordering from phase separation in a liquid-crystalline continuous phase, Nature (London) **407**, 611 (2000).
[7] J.-M. Choi, A. S. Holehouse, and R. V. Pappu, Physical principles underlying the complex biology of intracellular phase transitions, Annu. Rev. Biophys. **49**, 107 (2020).
[8] H. Tanaka, Viscoelastic phase separation in biological cells, Commun. Phys. **5**, 167 (2022).
[9] D. S. W. Lee, A. R. Strom, and C. P. Brangwynne, The mechanobiology of nuclear phase separation, APL Bioeng. **6**, 021503 (2022).
[10] A. Kumar and S. A. Safran, Fluctuations and shape dependence of microphase separation in systems with long-range interactions, Phys. Rev. Lett. **131**, 258401 (2023).
[11] D. Deviri and S. A. Safran, Mechanosensitivity of phase separation in an elastic gel, Eur. Phys. J. E **47**, 16 (2024).
[12] R. W. Style, T. Sai, N. Fanelli, M. Ijavi, K. Smith-Mannschott, Q. Xu, L. A. Wilen, and E. R. Dufresne, Liquid-liquid phase separation in an elastic network, Phys. Rev. X **8**, 011028 (2018).
[13] K. A. Rosowski, T. Sai, E. Vidal-Henriquez, D. Zwicker, R. W. Style, and E. R. Dufresne, Elastic ripening and inhibition of liquid-liquid phase separation, Nat. Phys. **16**, 422 (2020).
[14] K. A. Rosowski, E. Vidal-Henriquez, D. Zwicker, R. W. Style, and E. R. Dufresne, Elastic stresses reverse Ostwald ripening, Soft Matter **16**, 5892 (2020).

[15] S. Wilken, A. Chaderjian, and O. A. Saleh, Spatial organization of phase-separated DNA droplets, Phys. Rev. X **13**, 031014 (2023).

[16] J. X. Liu, M. P. Haataja, A. Košmrlj, S. S. Datta, C. B. Arnold, and R. D. Priestley, Liquid-liquid phase separation within fibrillar networks, Nat. Commun. **14**, 6085 (2023).

[17] X. Ren and L. Truskinovsky, Finite scale microstructures in nonlocal elasticity, J. Elast. **59**, 319 (2000).

[18] M. Kothari and T. Cohen, Effect of elasticity on phase separation in heterogeneous systems, J. Mech. Phys. Solids **145**, 104153 (2020).

[19] X. Wei, J. Zhou, Y. Wang, and F. Meng, Modeling elastically mediated liquid-liquid phase separation, Phys. Rev. Lett. **125**, 268001 (2020).

[20] P. Ronceray, S. Mao, A. Košmrlj, and M. P. Haataja, Liquid demixing in elastic networks: Cavitation, permeation, or size selection?, Europhys. Lett. **137**, 67001 (2022).

[21] S. Biswas, B. Mukherjee, and B. Chakrabarti, Thermodynamics predicts a stable microdroplet phase in polymer-gel mixtures undergoing elastic phase separation, Soft Matter **18**, 8117 (2022).

[22] J. Little, A. J. Levine, A. R. Singh, and R. Bruinsma, Finite-strain elasticity theory and liquid-liquid phase separation in compressible gels, Phys. Rev. E **107**, 024418 (2023).

[23] Y. Grabovsky and L. Truskinovsky, A class of nonlinear elasticity problems with no local but many global minimizers, J. Elast. **154**, 147 (2023).

[24] C. Fernández-Rico, S. Schreiber, H. Oudich, C. Lorenz, A. Sicher, T. Sai, V. Bauernfeind, S. Heyden, P. Carrara, L. D. Lorenzis, R. W. Style, and E. R. Dufresne, Elastic microphase separation produces robust bicontinuous materials, Nat. Mater. **23**, 124 (2024).

[25] T. Tanaka, S. Ishiwata, and C. Ishimoto, Critical behavior of density fluctuations in gels, Phys. Rev. Lett. **38**, 771 (1977).

[26] T. Tanaka, Dynamics of critical concentration fluctuations in gels, Phys. Rev. A **17**, 763 (1978).

[27] Y. Li and T. Tanaka, Study of the universality class of the gel network system, J. Chem. Phys. **90**, 5161 (1989).

[28] A. Onuki, Theory of phase transition in polymer gels, in *Responsive Gels: Volume Transitions I*, edited by K. Dušek (Springer, Berlin, 1993), pp. 63–121.

[29] H. Nishimori and A. Onuki, Pattern formation in phase-separating alloys with cubic symmetry, Phys. Rev. B **42**, 980 (1990).

[30] E. Vidal-Henriquez and D. Zwicker, Cavitation controls droplet sizes in elastic media, Proc. Natl. Acad. Sci. U.S.A. **118**, e2102014118 (2021).

[31] Y. Qiang, C. Luo, and D. Zwicker, Nonlocal elasticity yields equilibrium patterns in phase separating systems, Phys. Rev. X **14**, 021009 (2024).

[32] A. Eringen, C. Speziale, and B. Kim, Crack-tip problem in non-local elasticity, J. Mech. Phys. Solids **25**, 339 (1977).

[33] A. C. Eringen, Theory of nonlocal elasticity and some applications, Res Mech. **21**, 313 (1987).

[34] C. Polizzotto, P. Fuschi, and A. Pisano, A strain-difference-based nonlocal elasticity model, Int. J. Solids Struct. **41**, 2383 (2004).

[35] N. J. Derr, D. C. Fronk, C. A. Weber, A. Mahadevan, C. H. Rycroft, and L. Mahadevan, Flow-driven branching in a frangible porous medium, Phys. Rev. Lett. **125**, 158002 (2020).

[36] E. Skoruppa, A. Voorspoels, J. Vreede, and E. Carlon, Length-scale-dependent elasticity in DNA from coarse-grained and all-atom models, Phys. Rev. E **103**, 042408 (2021).

[37] M. Rubinstein and R. H. Colby, *Polymer Physics* (Oxford University Press, Oxford, 2003).

[38] F. Tanaka, *Polymer Physics: Applications to Molecular Association and Thermoreversible Gelation* (Cambridge University Press, New York, 2011).

[39] T. P. Lodge and P. C. Hiemenz, *Polymer Chemistry*, 3rd ed. (CRC Press, Boca Raton, FL, 2020).

[40] M. S. Dimitriyev, Y.-W. Chang, P. M. Goldbart, and A. Fernández-Nieves, Swelling thermodynamics and phase transitions of polymer gels, Nano Futures **3**, 042001 (2019).

[41] M. Doi, Gel dynamics, J. Phys. Soc. Jpn. **78**, 052001 (2009).

[42] See Supplemental Material at http://link.aps.org/supplemental/10.1103/5q7m-3fpn, which includes Refs. [43–68], for further details on (i) the material conservation relation [Eq. (6)] and the free energy [Eq. (7)], (ii) comparison with experiments and derivations of Eqs. (11) and (12), (iii) general phase diagrams, (iv) fluctuation effects and scattering, (v) universality of the scaling results, and (vi) numerical techniques.

[43] O. Gonzalez and A. M. Stuart, *A First Course in Continuum Mechanics* (Cambridge University Press, New York, 2008).

[44] W. H. Han, F. Horkay, and G. B. McKenna, Mechanical and swelling behaviors of rubber: A comparison of some molecular models with experiment, Math. Mech. Solids **4**, 139 (1999).

[45] J. F. Douglas and G. B. McKenna, The effect of swelling on the elasticity of rubber: Localization model description, Macromolecules **26**, 3282 (1993).

[46] G. B. McKenna, J. F. Douglas, K. M. Flynn, and Y. Chen, The "localization model" of rubber elasticity: Comparison with torsional data for natural rubber networks in the dry state, Polymer **32**, 2128 (1991).

[47] P. J. Flory, Statistical thermodynamics of random networks, Proc. R. Soc. A **351**, 351 (1976).

[48] H. M. James and E. Guth, Theory of the elasticity of rubber, J. Appl. Phys. **15**, 294 (1944).

[49] S. D. Reinitz, E. M. Carlson, R. A. Levine, K. J. Franklin, and D. W. Van Citters, Dynamical mechanical analysis as an assay of cross-link density of orthopaedic ultra high molecular weight polyethylene, Polym. Test. **45**, 174 (2015).

[50] A. Onuki, Theory of pattern formation in gels: Surface folding in highly compressible elastic bodies, Phys. Rev. A **39**, 5932 (1989).

[51] D. Jia and M. Muthukumar, Theory of charged gels: Swelling, elasticity, and dynamics, Gels **7**, 49 (2021).

[52] J. E. Mark, Some interesting things about polysiloxanes, Acc. Chem. Res. **37**, 946 (2004).

[53] S. Villain-Guillot and D. Andelman, The lamellar-disorder interface: One-dimensional modulated profiles, Eur. Phys. J. B **4**, 95 (1998).

[54] U. Thiele, T. Frohoff-Hülsmann, S. Engelnkemper, E. Knobloch, and A. J. Archer, First order phase transitions and the thermodynamic limit, New J. Phys. **21**, 123021 (2019).

[55] S. Komura and D. Andelman, Adhesion-induced lateral phase separation in membranes, Eur. Phys. J. E **3**, 259 (2000).

[56] P. M. Chaikin and T. C. Lubensky, *Principles of Condensed Matter Physics* (Cambridge University Press, New York, 1995).

[57] K. Yamada and S. Komura, The dynamics of order-order phase separation, J. Phys. Condens. Matter **20**, 155107 (2008).

[58] A. Onuki, Paradox in phase transitions with volume change, Phys. Rev. A **38**, 2192 (1988).

[59] S. Hirotsu, Softening of bulk modulus and negative Poisson's ratio near the volume phase transition of polymer gels, J. Chem. Phys. **94**, 3949 (1991).

[60] T. Koga, T. Koga, K. Kimishima, and T. Hashimoto, Long-range density fluctuations in a symmetric diblock copolymer, Phys. Rev. E **60**, R3501 (1999).

[61] S. Komura and N. Shimokawa, Dynamical Brazovskii effect, Soft Mater. **6**, 85 (2008).

[62] I. W. Hamley and V. E. Podneks, On the Landau–Brazovskii theory for block copolymer melts, Macromolecules **30**, 3701 (1997).

[63] J. M. Aguirregabiria, A. Hernández, and M. Rivas, δ-function converging sequences, Am. J. Phys. **70**, 180 (2002).

[64] A. Bray, Theory of phase-ordering kinetics, Adv. Phys. **43**, 357 (1994).

[65] D. J. Eyre, An unconditionally stable one-step scheme for gradient systems (unpublished).

[66] B. P. Vollmayr-Lee and A. D. Rutenberg, Fast and accurate coarsening simulation with an unconditionally stable time step, Phys. Rev. E **68**, 066703 (2003).

[67] S. Yoon, D. Jeong, C. Lee, H. Kim, S. Kim, H. G. Lee, and J. Kim, Fourier-spectral method for the phase-field equations, Mathematics **8**, 1385 (2020).

[68] https://github.com/manu-mannattil/elastomers

[69] F. Horkay and J. F. Douglas, Influence of solvent quality on the swelling and deswelling and the shear modulus of semi-dilute solution cross-linked poly(vinyl acetate) gels, J. Chem. Phys. **158**, 244901 (2023).

[70] A. Onuki and S. Puri, Spinodal decomposition in gels, Phys. Rev. E **59**, R1331 (1999).

[71] A. Onuki, *Phase Transition Dynamics* (Cambridge University Press, Cambridge, England, 2002).

[72] T. Yamaue, T. Taniguchi, and M. Doi, Shrinking dynamics and patterns of gels, AIP Conf. Proc. **519**, 584 (2000).

[73] T. Yamaue, T. Taniguchi, and M. Doi, The simulation of the swelling and deswelling dynamics of gels, Mol. Phys. **102**, 167 (2004).

[74] Y. Rabin and A. Onuki, Osmotic and longitudinal moduli of polymer gels, Macromolecules **27**, 870 (1994).

[75] J. F. Doyle, *Wave Propagation in Structures*, 3rd ed. (Springer, New York, 2021)

[76] Q. Liu, T. Ouchi, L. Jin, R. Hayward, and Z. Suo, Elastocapillary crease, Phys. Rev. Lett. **122**, 098003 (2019).

[77] R. M. Hornreich, M. Luban, and S. Shtrikman, Critical behavior at the onset of $\vec{k}$-space instability on the λ line, Phys. Rev. Lett. **35**, 1678 (1975).

[78] A. Onuki, Phase transition in deformed gels, J. Phys. Soc. Jpn. **57**, 699 (1988).

[79] R. J. Gaylord and J. F. Douglas, Rubber elasticity: A scaling approach, Polym. Bull. **18**, 347 (1987).

[80] R. J. Gaylord and J. F. Douglas, The localisation model of rubber elasticity. II, Polym. Bull. **23**, 529 (1990).

[81] J. F. Douglas, The localization model of rubber elasticity, Macromol. Symp. **291**, 230 (2010).

[82] J. F. Douglas and F. Horkay, Influence of swelling on the elasticity of polymer networks cross-linked in the melt state: Test of the localization model of rubber elasticity, J. Chem. Phys. **160**, 224903 (2024).

[83] T. Canal and N. A. Peppas, Correlation between mesh size and equilibrium degree of swelling of polymeric networks, J. Biomed. Mater. Res. **23**, 1183 (1989).

[84] S. H. Yoo, C. Cohen, and C.-Y. Hui, Mechanical and swelling properties of PDMS interpenetrating polymer networks, Polymer **47**, 6226 (2006).

[85] E. Parrish, M. A. Caporizzo, and R. J. Composto, Network confinement and heterogeneity slows nanoparticle diffusion in polymer gels, J. Chem. Phys. **146**, 203318 (2017).

[86] N. R. Richbourg and N. A. Peppas, The swollen polymer network hypothesis: Quantitative models of hydrogel swelling, stiffness, and solute transport, Prog. Polym. Sci. **105**, 101243 (2020).

[87] S. Leibler and D. Andelman, Ordered and curved mesostructures in membranes and amphiphilic films, J. Phys. II (France) **48**, 2013 (1987).

[88] M. A. Wisniewska, J. G. Seland, and W. Wang, Determining the scaling of gel mesh size with changing crosslinker concentration using dynamic swelling, rheometry, and PGSE NMR spectroscopy, J. Appl. Polym. Sci. **135**, 46695 (2018).

[89] Y. Tsuji, X. Li, and M. Shibayama, Evaluation of mesh size in model polymer networks consisting of tetra-arm and linear poly(ethylene glycol)s, Gels **4**, 50 (2018).

[90] M. Seul and D. Andelman, Domain shapes and patterns: The phenomenology of modulated phases, Science **267**, 476 (1995).

[91] D. Andelman and R. E. Rosensweig, Modulated phases: Review and recent results, J. Phys. Chem. B **113**, 3785 (2009).

[92] L. Leibler, Theory of microphase separation in block copolymers, Macromolecules **13**, 1602 (1980).

[93] G. H. Fredrickson and E. Helfand, Fluctuation effects in the theory of microphase separation in block copolymers, J. Chem. Phys. **87**, 697 (1987).

[94] T. Garel and S. Doniach, Phase transitions with spontaneous modulation-the dipolar Ising ferromagnet, Phys. Rev. B **26**, 325 (1982).

[95] D. Andelman, F. Broçhard, and J.-F. Joanny, Phase transitions in Langmuir monolayers of polar molecules, J. Chem. Phys. **86**, 3673 (1987).

[96] K. R. Elder and M. Grant, Modeling elastic and plastic deformations in nonequilibrium processing using phase field crystals, Phys. Rev. E **70**, 051605 (2004).
[97] N. Provatas and K. Elder, *Phase-Field Methods in Materials Science and Engineering* (Wiley-VCH, Weinheim, 2011).
[98] R. M. Briber and B. J. Bauer, Effect of crosslinks on the phase separation behavior of a miscible polymer blend, Macromolecules **21**, 3296 (1988).
[99] D. J. Read, M. G. Brereton, and T. C. McLeish, Theory of the order-disorder phase transition in cross-linked polymer blends, J. Phys. II (France) **5**, 1679 (1995).
[100] P. G. de Gennes, Effect of cross-links on a mixture of polymers, J. Phys. Lett. **40**, 69 (1979).
[101] S. A. Brazovskii, Phase transition of an isotropic system to a nonuniform state, Sov. Phys. JETP **41**, 85 (1975).
[102] F. S. Bates, W. Maurer, T. P. Lodge, M. F. Schulz, M. W. Matsen, K. Almdal, and K. Mortensen, Isotropic Lifshitz behavior in block copolymer-homopolymer blends, Phys. Rev. Lett. **75**, 4429 (1995).
[103] F. S. Bates, W. W. Maurer, P. M. Lipic, M. A. Hillmyer, K. Almdal, K. Mortensen, G. H. Fredrickson, and T. P. Lodge, Polymeric bicontinuous microemulsions, Phys. Rev. Lett. **79**, 849 (1997).
[104] M. Teubner and R. Strey, Origin of the scattering peak in microemulsions, J. Chem. Phys. **87**, 3195 (1987).
[105] S. Komura, Mesoscale structures in microemulsions, J. Phys. Condens. Matter **19**, 463101 (2007).
[106] Y. Li, G. Wang, and Z. Hu, Turbidity study of spinodal decomposition of an *n*-isopropylacrylamide gel, Macromolecules **28**, 4194 (1995).
[107] Y. Zhao, T. Hashimoto, and J. F. Douglas, Frustrating the lamellar ordering transition of polystyrene-block-polyisoprene with a C_{60} additive, J. Chem. Phys. **130**, 124901 (2009).
[108] S. Ghosh, A. Mukherjee, R. Arroyave, and J. F. Douglas, Impact of particle arrays on phase separation composition patterns, J. Chem. Phys. **152**, 224902 (2020).
[109] S. Ghosh and J. F. Douglas, Phase separation in the presence of fractal aggregates, J. Chem. Phys. **160**, 104903 (2024).
[110] K. Dušek and M. Dušková-Smrčková, Volume phase transition in gels: Its discovery and development, Gels **6**, 22 (2020).
[111] M. Mussel, P. J. Basser, and F. Horkay, Ion-induced volume transition in gels and its role in biology, Gels **7**, 20 (2021).